Biomedical Microdevices (2021) 23:31
https://doi.org/10.1007/s10544-021-00567-y

Smartphone enabled miniaturized temperature controller platform to synthesize NiO/CuO nanoparticles for electrochemical sensing and nanomicelles for ocular drug delivery applications

Madhusudan B Kulkarni[1] · K Velmurugan[2] · Enaganti Prasanth[1] · Khairunnisa Amreen[1] · Jayabalan Nirmal[2] · Sanket Goel[1]

Accepted: 31 May 2021

Abstract
Undoubtedly, various kinds of nanomaterials are of great significance due to their enormous applications in diverse areas. The structure and productivity of nanomaterials are heavily dependent on the process used for their synthesis. The synthesizing process plays a vital role in shaping nanomaterials effectively for better productivity. The conventional method requires expensive and massive thermal instruments, a huge volume of reagents. This paper aims to develop an Automatic Miniaturized Temperature Controller (AMTC) device for the synthesis of nickel oxide (NiO), copper oxide (CuO) nanoparticles, and nanomicelles. The device features a low-cost, miniaturized, easy-to-operate with plug-and-play power source, precise temperature control, and geotagged real-time data logging facility for the producing nanoparticles. With a temperature accuracy of ± 2 °C, NiO and CuO nanoparticles, and nanomicelles are synthesized on AMTC device, and are subjected to different characterizations to analyze their morphological structure. The obtained mean size of NiO and CuO is 27.14 nm and 85.13 nm respectively. As a proof-of-principle, the synthesized NiO and CuO nanomaterials are validated for electrochemical sensing of dopamine, hydrazine, and uric acid. Furthermore, the study is conducted, wherein, Dexamethasone (Dex) loaded nanomicelles are developed using AMTC device and compared to the conventional thin-film hydration method. Subsequently, as a proof-of-application, the developed nanomicelles are evaluated for transcorneal penetration using exvivo goat cornea model. Ultimately, the proposed device can be utilized for performing a variety of controlled thermal reactions on a minuscule platform with an integrated and miniaturized approach for various applications.

Keywords Electrochemical sensing · Automatic temperature controller (AMTC) · Nanoparticles (NPs) · Nickel oxide (NiO) · Copper oxide (CuO) · Dex loaded nanomicelles · Trans corneal diffusion · Ocular drug delivery

1 Introduction

Recently, nano-sized materials such as nanotubes, nanowires, nanoparticles, and nanomicelles manifest novel properties that are considerably distinct from those of discrete molecules and atoms, or bulk materials (Jamkhande et al. 2019; Ndolomingo et al. 2020). Due to these reasons, many researchers are working persistently to develop several competent techniques to produce superior quality nanoparticles leading to numerous applications in various fields like biomedical, industrial, environmental, and food agriculture (Ealias and Saravanakumar 2017; Mohan et al. 2020). The curiosity in the synthesis of nanomaterials has grown drastically due to their precise chemical, structural, and physical properties (Kulkarni and Goel 2020a), leading to the production of nanomaterials with definite size and structure (Powar and Patel 2019) and dimension (Silva et al. 2019). Such nanomaterials can be used extensively in various research areas such as imaging, catalysis, data storage, sensing, drug delivery, and bacterial analysis (Wang et al. 2017; Puneeth et al. 2021). The conventional method for the synthesis of

✉ Sanket Goel
sgoel@hyderabad.bits-pilani.ac.in

[1] MEMS, Microfluidics and NanoElectronics (MMNE) Lab, Department of Electrical and Electronics Engineering, Birla Institute of Technology and Science (BITS) Pilani, Hyderabad Campus, Hyderabad 500078, Telangana, India

[2] Translational Pharmaceutics Research Laboratory (TPRL), Department of Pharmacy, Birla Institute of Technology and Science (BITS) Pilani, Hyderabad Campus, Hyderabad 500078, Hyderabad, Telangana, India

Published online: 06 June 2021

nanomaterials suffers from the slow response and the need for autoclaves and heavy thermal instruments. Moreover, such methods hamper from being expensive, arduous, and time-consuming, which leads to rendering the process unprofitable for smaller quantities (Yang and Park 2019).

Nickel oxide (NiO) nanomaterials showcase a significant evolution of metal oxide with a spherical lattice structure (Ni et al. 2012). It has increased the attention due to their potential use in a diversity of applications like batteries (Feng et al. 2014), supercapacitors (Li et al. 2018), catalysis (U.S, J., Goel, S. 2020), fuel cell (Dector et al. 2021), and gas sensors (Thota and Kumar 2007). It exhibits excellent durability and electrochemical stability (Saravanan et al. 2013). With a broad-band gap of 3.6—4 eV, a NiO semiconductor has become an important candidate for various applications like solar cells (Meneses et al. 2007). The NiO nanomaterials are typically produced by the co-precipitation technique using divergent precursors (Ekeroth et al. 2019; Chopra et al. 2010). Similarly, copper oxide (CuO) nanomaterials have increased considerable attention due to their excellent magnetic, electrical, physical, optical properties, and have an extensive range of applications in biological, biomedical, and industrial fields (Phiwdang et al. 2013; Pandey et al. 2012). Evidently, these properties can be further enhanced by selecting an appropriate synthesizing method, as it can regulate the size, shape, and morphology of the nanomaterials. Various nanostructures of CuO have been produced in the form of the nanorod, nanowire, nanoneedle, nanomicelles, nanoflakes, nano-flower, and nanospheres, and nanobullets (Maqbool et al. 2017). Numerous approaches have been projected to synthesize CuO nanoparticles with distinct methods like sonochemical (Kesavan and Chen 2020), quick precipitation (Batool and Valiyaveettil 2020), and thermal oxidation (Kulkarni et al. 2020). The hydrothermal method is common and mostly used for synthesizing nanoparticles as a traditional approach. Mainly the traditional nanomaterial synthesis suffers due to uncontrolled time for mixing with a delayed response (Dobrucka et al. 2021). Besides, traditional processing needs the groundwork of particles in mass production leading to the huge prerequisite of valuable and expensive materials and distinct types of equipment (Li et al. 2020). Hence, there is a need to automate and integrate a method to synthesize the nanoparticles with low thermal power and energy, inexpensive and fast response time for small-scale production, and good yield (Qu et al. 2020; Shi and Chopra 2011).

Micelles, with an exceptional drug-entrapment capacity, have a smaller size and easy formulation. Nanomicelles are commonly utilized for the formulation of pure aqueous solutions to load poorly water-soluble drugs, which are created using amphiphilic molecules (Vadlapudi and Mitra 2013). Moreover, nanomicellar formulations can also improve drug availability in ocular tissues, representing better therapeutic outcomes (Patel et al. 2015). Several researchers are focussing on the development of nanomicellar formulations for ocular use and studies have been carried out to examine the potentials of the ocular nanomicelle application to treat various ocular diseases (Vadlapudi et al. 2014; Patel 2013). Nanomicelles are proven to be a good method for the ocular delivery of especially hydrophobic drugs (Omerovi and Vrani 2020). They offer numerous advantages, like corneal penetration, ocular biocompatibility, ease of sterilization. Further, the nanomicelles improve the bioavailability of the hydrophobic drugs due to the nano-size of drug particles, precorneal retention time, stability, and utilization of various polymers and surfactants (Alami-Milani et al. 2019).

Ocular structures possess various barriers to prevent xenobiotics including therapeutic drugs to reach various tissues of the eye, thus reduce the ocular bioavailability of various drugs (Gote et al. 2019). The barriers comprise of both static (corneal epithelium, corneal stroma, corneal endothelium) and dynamic barriers (tear dilution, conjunctival, blood-aqueous barrier, and retinal-blood barriers) (Chrai et al. 1974). These barriers provide challenges for the topically administered drugs to achieve optimum therapeutic concentrations at the targeted therapeutic site in the anterior and posterior segment (Nirmal et al. 2013a, 2013b).

To synthesize various nanomaterials, such as NiO and ZnO nanomaterials, and nanomicelles, a miniaturized arduino pro-mini microcontroller-based temperature controller platform, with precise temperature controlling capability, can lead to distinguished and notable results, and find application in numerous areas. These include diagnostics of various diseases, screening of drugs, electrochemical, drug delivery, tissue engineering, biomedical imaging, bacterial process, and droplet-based approach for biosensing (Chaipan et al. 2017; Kulkarni and Goel 2020b). A smaller volume of the sample permits a precise solution transferal on the microchannel reservoir and this technology has newly grown as an important milestone to synthesize nanoparticles (Islam et al. 2018). The role of reaction temperature has influenced greatly on particle size and shape, with lower temperatures resulting in more and thinner particles with a greater surface area than those produced at higher temperatures (Jiang et al. 2011). High temperatures can induce the formation of different crystalline phases with different characteristics. The size of the particle is also greatly dependent on various factors such as pH, reagents, the process of operation, reaction temperature and time, and further, the inclusion of purification steps like sonication and centrifugation all these play a role in determining the physical characteristics and stability of nanoparticle formation (Liu et al. 2020; Sigwadi et al. 2017).

These days, a temperature controller platform has become very indispensable and plays a crucial role in many fields of study. Its emergent applications can be seen in many household appliances for cooling and heating applications,

biomedical, biochemical, industrial automation, process control stations, food industries, and pharmaceutics (Kamaly et al. 2012). PID (proportional integral derivative) based temperature controller is widely used due to its accurateness and constancy, whereby PID can be implemented using the open-source library function available in off-the-shelf microcontroller like Arduino IDE (Hamid et al. 2009). It is extremely effective and efficient in upholding the required temperature despite swift changes in ambient thermal conditions, offering more exactness and reliability than classical on/off controllers (Asraf et al. 2017). Therefore, a cost-effective, low-powered, portable Automatic Miniaturized Temperature Controller (AMTC) is realized using fewer electronic modules such as a microcontroller, customized switching circuitry with BJT and MOSFET, and Bluetooth/IoT for real-time data analysis for regulating, manipulating, and monitoring the temperature data. Conventional temperature controller devices such as hot air oven, boiler, and muffle furnace are widely used for traditional nanoparticle synthesis. These benchtop devices are bulky, require human intervention, dissipates more thermal loss, and are quite expensive (Park et al. 2020). Table. 1 summarize the difference between existing conventional-based temperature controller devices used for nanoparticle synthesis and various AMTC systems for synthesizing the nanomaterials and nanomicelles in a micro-scale platform.

The present work describes the development of an economical, integrated, and miniaturized AMTC platform which can be easily used for the synthesis of several nanoparticles and nanomicelles. Here, as a proof-of-principle, the synthesis of nickel oxide (NiO), copper oxide (CuO) nanoparticles, and Dex loaded nanomicelles were carried out on an AMTC device. An Arduino pro-mini microcontroller was realized which acted as the main chip by controlling and monitoring the heaters and sensors which are integrated on the printed circuit board. The FESEM and EDX characterization for synthesized NiO and CuO nanoparticles were executed to study and investigate the morphology and elemental composition. Further, nanomicelles characterization and its application for ocular-based drug delivery were carried out using this proposed system. The FESEM and EDX characterization revealed the formation of the nanostructures for both NiO and CuO. Further, the produced NiO nanoparticles were used for electrocatalyst sensing of uric acid and hydrazine, and CuO nanomaterials were used for electrocatalyst sensing of uric acid and dopamine respectively. Furthermore, as a proof-of-application, the developed nanomicelles were evaluated for transcorneal penetration using exvivo goat cornea model.

2 Experimental

2.1 Automatic temperature controller (AMTC) module

The AMTC system plays an indispensable role in nanoparticle synthesis, where it is crucial to provide a quick and precise temperature. Figure 1a shows a block diagram that includes a microcontroller, driving and switching circuit, cartridge heater, and thermocouple sensor (k-type). In this device, a smaller microcontroller in the family of arduino, Arduino pro-mini 328 ($18\times33mm^2$), has been incorporated. The low-cost and miniaturized arduino pro-min supports auto-reset, 14 digital input/output pins, and 6 analog input pins. Pro-mini works on 5 V/16 MHz and maximum output current of has an in-built library for proportional-derivative-integral (PID) controller making it a more precise temperature controller module. In this work, an Arduino IDE (www.arduino.cc) with open-source software was used for coding the instructions. Arduino pro mini is accountable for regulating, coordinating, manipulating, and monitoring the device.

The DC-DC buck convertor (LM2596) breakout module can be set to the desired voltage at the output (load) by step down voltage from its applied input voltage. From an adapter (12 V/3.75A), it can be directly connected to the buck converter where 5 V DC is achieved and fed to power the arduino pro mini. Figure 1b shows a schematic diagram

Table. 1 Comparison between a conventional controller and microfluidic AMTC system

Approach	Conventional based temperature controller			Microfluidic based temperature controller		
Parameters	Hot air oven (Wang et al. 2013)	Muffle furnace (Lu et al. 2011)	Boiler (Yan et al. 2015)	Hot plate (Lee et al. 2009)	Oil Bath (Nightingale and Mello 2009)	Cartridge heater (Nakayama et al. 2006)
Temperature range	800 °C	1600 °C	550 °C	350 °C	200 °C	250 °C
Accuracy	±1 °C	±2 °C	±5 °C	±2 °C	±3 °C	±2 °C
Heat dissipation	More	More	Medium	Medium	Low	Low
Power consumption	1200 W	1520 W	1000 W	800 W	500 W	38 W
Cost	Expensive	Costly	Average	Costlier	Average	Cheaper
Size	Bulky	Heavy	Hefty	Small	Medium	Miniature

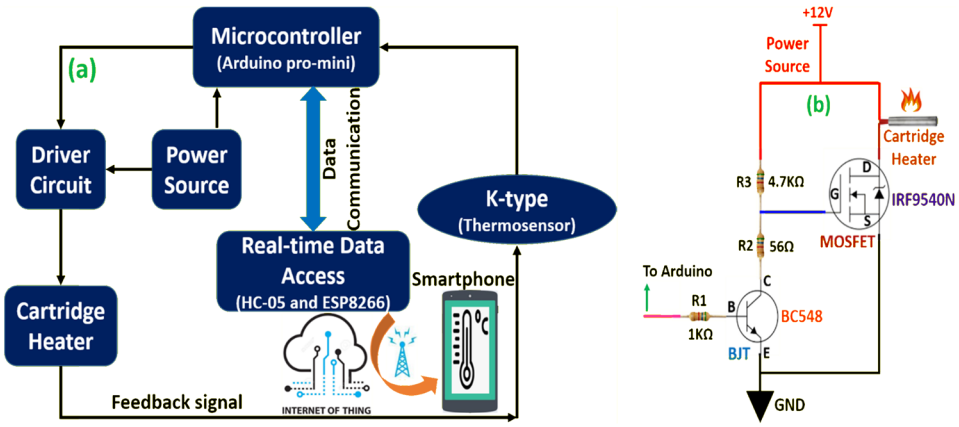

Fig. 1 (**a**) A simple block diagram of the AMTC system (**b**) Schematic of self-developed switching circuitry

of self-developed switching circuitry that was designed and developed for executing the regular switching operation to have control over current flow in a driver circuit, without the need for manual cutting or splice of the power source wires. Hereby, the switching circuit was designed with a basic bipolar transistor (BC548), power MOS-field effect transistor (IRF9540N), and limiting resistors (Kulkarni et al. 2021). This takes care of the current flowing across the heater and switches accordingly following the arduino instructions. The microcontroller triggers the signal in boolean logic (0 and 1) through pulse width modulation (PWM) which is associated with the base pin of the bipolar transistor (BJT). Gate terminal of field-effect transistor (FET) was connected to 12 V DC via limiting resistors. The drain terminal was connected to one end of the heater and another end of the heater is connected to 12 V DC. Thus, the overall switching was operated by these aforementioned transistors. A circular tube-shaped cartridge heater ($25 \times 3 mm^2$), coated with stainless steel material of higher grade, was used for the heating process. The cartridge heater is a voltage-controlled device with a power rating of 38 W, wherein the amount of current required to drive is very minimal, and a good ramping rate was calibrated with temperature and time.

Figure 2 shows a schematic representation of the arduino pro-mini-based AMTC system. A k-type thermocouple sensor was used for manipulating and recording the desired temperature across the heater connected to arduino pro-mini and acts as a feedback signal. It has many advantages like a wide temperature measuring range, reliability, stability, precision, and smaller size. The MAX6675 is a breakout module that was used with the thermocouple responsible to reduce the error, fluctuation, and noise of the sensing signal. It operates at a 5 V power source and has full-duplex Serial Peripheral Interface (SPI) standards allowing the master

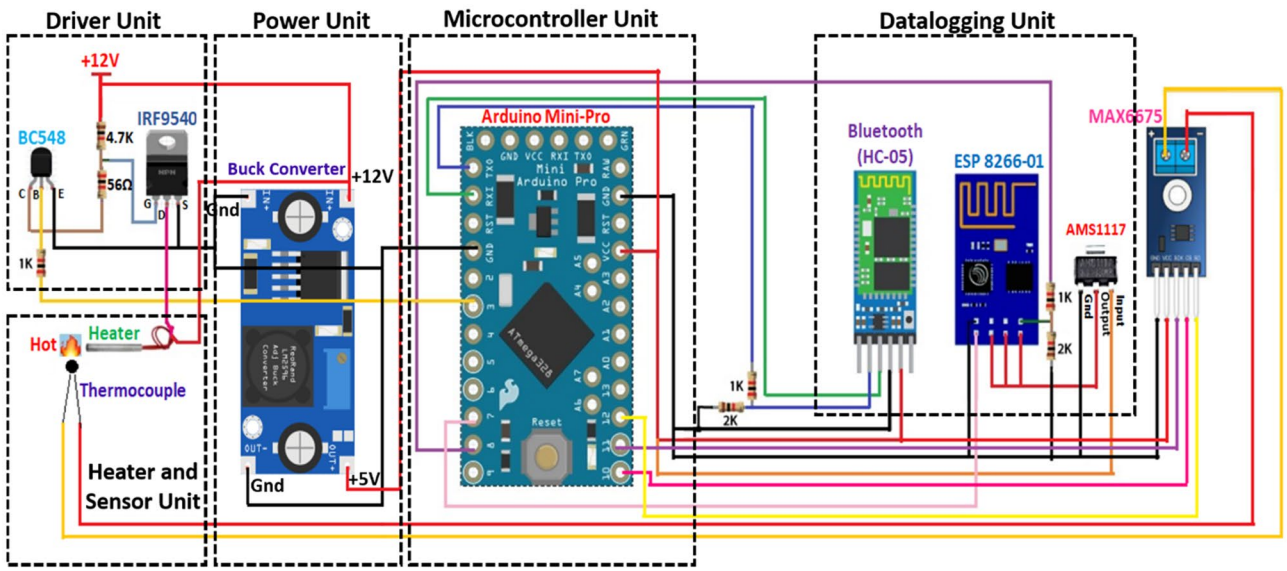

Fig. 2 Schematic diagram for Arduino pro-mini based AMTC system

and slave to send the data simultaneously. Here, arduino provides a simple method of tuning all PID terms (Proportional (K_P), Integral (K_I), and Derivative (K_D)). The PID controller has feedback control that delivers a good output performance stability perceived by considering optimized values such as $K_P = 160$, $K_I = 1$, and $K_D = 80$ as per the prerequisite with very low tolerance. Herein, the PID controller controls the temperature, executes the upper and lower limits within ± 2 °C. The device consists of Bluetooth and geotagging-based data logging features making it easier for data acquisition and data storage. The real-time data can be directly analyzed and stored on a smartphone through the open-source app and ThingSpeak permits users to collective, analyze, and visualize live data streaming facilities.

2.2 Chemicals and apparatus

The chemical used for the experimentation, uric acid, hydrazine, dopamine, Multi-walled carbon nanotube (MWCNT), Nickel nitrate, copper chloride, ascorbic acid, and urea, were purchased from Sigma Aldrich. Dexamethasone, Tocopherol Poly (ethylene glycol) 1000 Succinate (TPGS) and poloxamer P407, Acetonitrile. OrigaLsys Electrochem (OrigaFlex 500) instrument was used for the electrochemical sensing of uric acid, hydrazine, and dopamine. Dynamic light scattering (DLS) technique (Nano ZS 90, Malvern Instruments Ltd., UK), High-Pressure Liquid Chromatography (HPLC), Sonicator (GT Sonic ultra-sonic cleaner (China), Franz diffusion cell apparatus (PermeGear Inc., USA).

2.3 Synthesis of NiO, CuO Nanoparticles, and Nanomicelles

2.3.1 Preparation of NiO nanoparticles

The precursor's nickel nitrate ($Ni(NO_3)_2$) and urea (CH_4N_2O) were prepared in the ratio of 1:2 concentrations. The precursor was dissolved in DI water of volume 2 ml. The solution was well stirred using a magnetic stirrer for 15 min and then 2 ml of the reaction was poured onto 5 ml of a small borosil beaker, subsequently placed on the heating block. Further, it was heated from atmospheric thermal conditions to 180 °C for 60 min. The obtained green-colored powder was washed with DI water several times using the filtration method and kept in the oven for drying the powder at 65 °C for 3 h.

2.3.2 Preparation of CuO nanoparticles

The preparation of copper oxide was carried out by a conventional chemical precipitation process. Copper chloride and ascorbic acid precursors were taken in the ratio of 4:1 concentration and added in 4 ml DI water and sonicated for 30 min. The 3 ml of the reaction was transferred to a small petri dish (D = 50 mm) which was positioned on the heater and the pH value was measured and maintained neutral. The solution was kept at 75 °C for 3 h, thereby obtaining a light-brownish-colored product.

2.3.3 Preparation of nano-micelles

The Nanomicelle formulation of Dex was prepared by thin-film hydration method using: (i) Formulation preparation and solvent evaporation (ii) Rehydration. Further, Dexamethasone (0.1%) was accurately weighed and dissolved in Acetonitrile. Then, Tocopheryl Polyethylene Glycol Succinate (TPGS) (3%) and Poloxamer 407 (0.1%) were weighed and dissolved separately in Acetonitrile. These two solutions were then mixed and vortexed for few minutes to get a homogeneous solution. Here, 3 ml of Acetonitrile was used to dissolve the drug completely. 3 ml of Phosphate-buffered solution was taken for final formulation. As a routine practice, this can be evident from various literature (Cholkar et al. 2014; Mandal et al. 2017; Velpandian et al. 2021), that specifies only to quantify the drugs and not the excipients.

The transcorneal penetration studies were performed using goat cornea using the franz diffusion apparatus. HPLC is used to analyze the concentration of the drug in the sample. The goat eyes were purchased from a butcher shop and the cornea was isolated from the whole eye. The removed cornea was washed with PBS buffer pH 7.4 and mounted between the donor and acceptor chamber of the diffusion cell. The acceptor compartment was filled with PBS buffer pH 7.4 and the temperature was maintained at 37 °C with stirring using a magnetic stirrer at 100 rpm throughout the study. The donor compartment was filled with Dex formulation. The samples were collected from the sample port of the franz diffusion apparatus using a syringe at time points 5, 15, 30, 60, 120, and 240 min respectively, and replaced with the same amount of PBS buffer pH 7.4. The collected samples were stored at -20 °C until analysis using HPLC. The circle-shaped cornea was dissected from the goat eye and the thickness of the cornea was measured using a digital micrometer before every experiment to maintain the average thickness of the cornea for various diffusion cells for transcorneal penetration studies and the average thickness was around 0.724 mm. The diameter of the goat cornea was around 17 mm. Goat cornea, pH 7.4 buffer, digital micrometer, and hamilton syringe were used for the exvivo study. Inspite of exvivo studies remains as an efficient tool to understand the transcorneal penetration of drugs and formulations, the model cannot imitate the factors like tear drainage and blinking latency which is found in the human eye.

Further, the resultant reaction mixture was kept on the self-designed AMTC system to execute the proposed method, and also, conventional rotatory evaporator method was carried out, to evaporate the solvent completely, later the

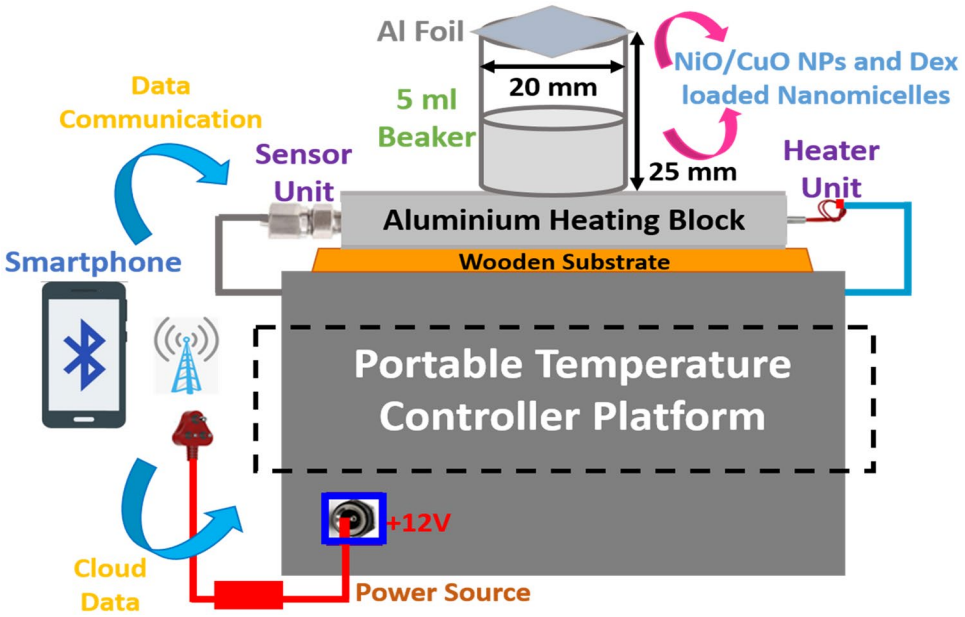

Fig. 3 Overview of a smartphone-enabled synthesis of nanoparticle on a portable heating device

obtained dry thin film was rehydrated with Phosphate Buffer Solution (PBS) pH 7.4 and sonicated for 5 min. Meanwhile, the process was carried out for the preparation of placebo nanomicelles without Dex.

2.4 Experimentation

Figure 3 shows an overview of smartphone-enabled nanoparticle synthesis on a portable heating device. The portable temperature controller module includes a microcontroller, DC buck converter, a switching circuit, cartridge heater, and sensor. The experimentation setup also shows the aluminium heating block ($50 \times 15 \times 10$ mm^3) used for heating. Both heater and sensor were inserted into the opposite ends of the block. The complete device was powered up by the 12 V/3A adapter. The 5 ml small beaker was kept on the heating block covered with the thin aluminium foil of thickness 11 µm. The real-time temperature data was made available directly on the smartphone through Bluetooth module (HC-05) and IoT (ESP 8266–01) breakout module using an open-source app. Hence, continuous data analysis and data storage can be observed and maintained easily.

3 Results and discussion

3.1 Heating process for synthesis of nanoparticle

Figure 4a shows the top-view of the temperature controller device. The heater output was controlled by the microcontroller and the thermocouple was used as a feedback

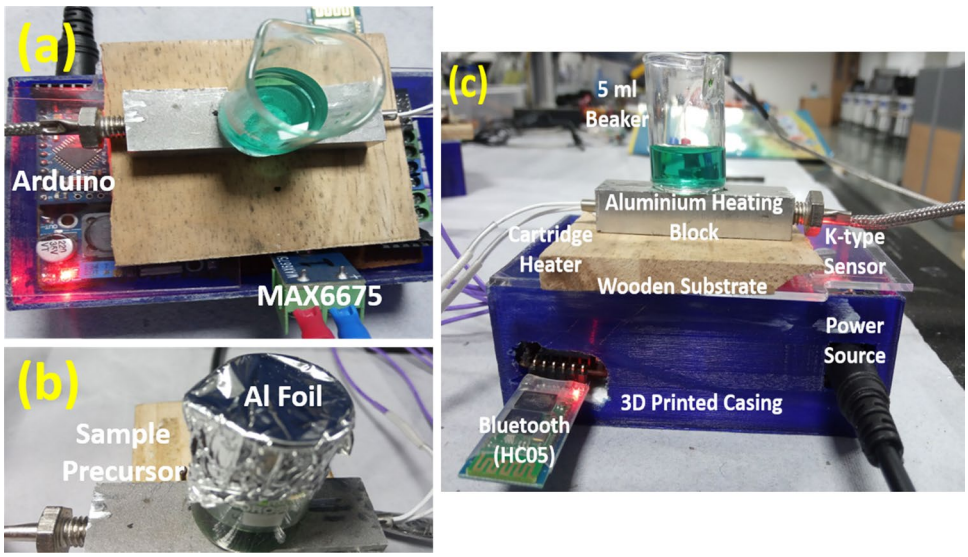

Fig. 4 (**a**) Top-view of temperature controller device (**b**) A 5 ml beaker with solution placed on a heating block covered with Al Foil (**c**) Complete 3D printed casing of heating module

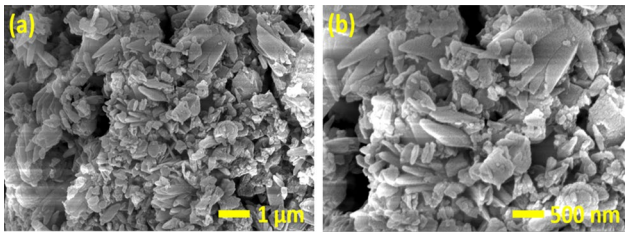

Fig. 5 SEM images of synthesized Nickel oxide (NiO) nanoparticles appears to be spherical shape nanostructures at a magnification rate (**a**) 60,000x (**b**) 300,000x

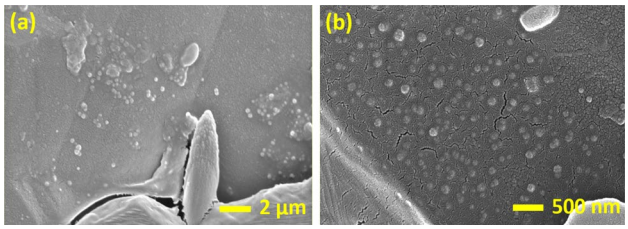

Fig. 6 SEM images of synthesized Copper oxide (CuO) nanoparticles appears to be spherical shaped nanostructures at a magnification rate (**a**) 25,000x (**b**) 120,000x

sensor for monitoring the temperature. The thermocouple sensor has a 12-bit resolution and can provide temperature measurements from 0 °C to 1024 °C with a precision of 0.25 °C. The sensor acted as a feedback response connected to arduino pro-mini by sending the continuous sensor data for temperature monitoring. The accuracy of the temperature controller was around ± 2 °C. The data logging is very simpler with continuous analysis and accessing of the temperature values on the smartphone. All the electronic modules were integrated and soldered on to single 3.93'(L) by 2.36'(W) of a printed circuit board ($99.8 \times 59.9 mm^2$). Figure 4b shows a 5 ml beaker with solution placed on a heating block covered with Al Foil. The dimensions of the complete device with 3D printed casing were 100 (L) × 60 (W) × 32 mm^3 (H) respectively. The smartphone-enabled data accessing and data recording is easier-to-use, faster, and simple. Figure 5c shows the complete 3D printed casing of the heating module.

3.2 Characterization of the NiO and CuO nanoparticle

3.2.1 NiO nanoparticle

The synthesized NiO nanoparticles were studied to understand the surface morphological features by the field emission scanning electron microscope (FESEM). The obtained images specify the presence of synthesized NiO nanomaterials, which appeared to be spherical with magnification up to 300 nm as shown in Fig. 5a. Further, it can be observed that the nanoparticles are greatly agglomerated and appear to be a cluster of NiO nanoparticles. The prepared NiO nanomaterials have an average diameter of 27.14 nm as shown in Fig. 5b. The NiO nanoparticles were synthesized at 450° calcination temperature and the obtained results were studied to recognize the potential of the projected method. The results were benchmarked with the literature which shows comparable results with an average diameter of 32.9 nm produced through the sol–gel method (Wardani et al. 2019).

3.2.2 CuO nanoparticle

The SEM images of the synthesized CuO nanoparticles were observed with agglomerated nanospheres structures with an average diameter of 85.13 nm. Figure 6a, b shows the SEM images which describe the structural and surface morphologies of the formed CuO. The characterization outcome illustrates the substantial presence of major elements of nanoparticles and further, these were compared with the traditional methods (Singh 2016).

To analyze the elemental composition existing in produced NiO and CuO nanomaterials, Energy-dispersive X-ray spectroscopy (EDX) was studied. Table 2 shows the EDX analysis, the statistical results show the percentage of content of major elements of NiO and CuO respectively. Energy-dispersive X-ray spectroscopy (EDX) is an analytical method utilized for the chemical composition or elemental analysis of a reaction mixture. It depends on the examination of an interaction of some basis of X-ray excitation and a reaction n mixture.

Further, Fig. 7a, b show the EDX spectrum for key elements of Ni, O for NiO nanoparticles, and Cu, O, and C elements for CuO nanoparticles.

Figure 8a, b show the size distribution curve of NiO and CuO nanomaterials respectively. Further, the sizes of NiO and CuO nanoparticles were examined naturally with ImageJ software (www.imagej.net), an open-source platform, for the examining of nanomaterials used to identify

Table 2 EDX Analysis of Key Elements of NiO and CuO

Elements	Weight(%)	Atomic(%)	Elements	Weight(%)	Atomic(%)
Oxygen	34.99	66.38	Oxygen	51.12	52.86
Nickel	65.01	33.62	Carbon	30.80	42.43
			Copper	18.08	4.71

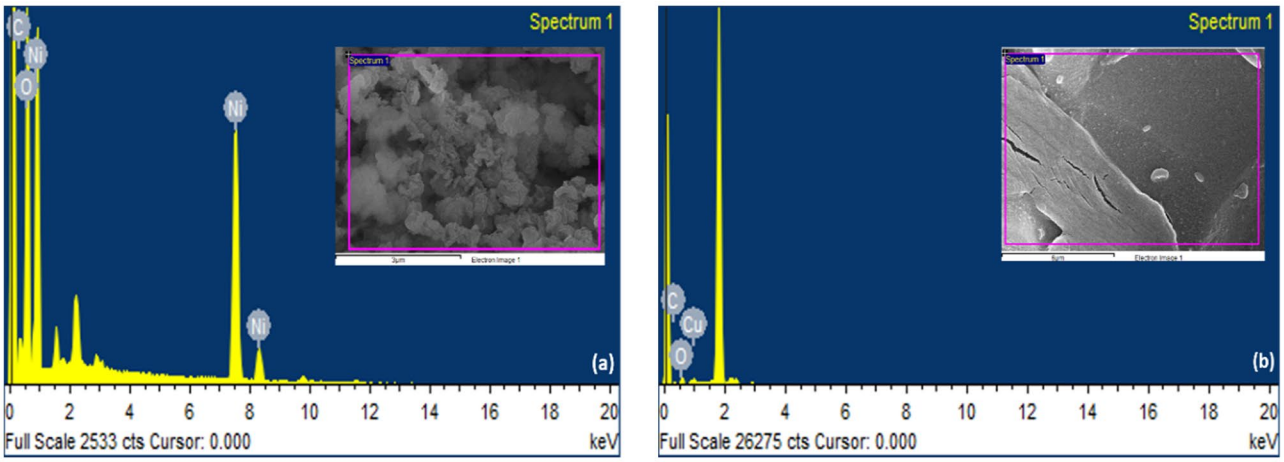

Fig. 7 (**a**) Processing of the EDX spectrum for Ni, O elements (**b**) Processing of the EDX spectrum for Cu, O, and C elements

the size distribution curve. Based on the obtained results from FESEM, the mean nanoparticle size (wc) and standard deviation (σ) were calculated.

3.2.3 Dex loaded nanomicelles for ocular drug delivery application

Dex-loaded nanomicelles were prepared by utilizing both conventional methods based on standard thin-film rehydration and the proposed AMTC system. Herein, the obtained parameters, such as particle size and zeta potential of Dex-loaded nanomicelles (0.1%), were determined by the Dynamic Light Scattering (DLS) technique, after filtering with 0.45 µm sterile nylon membrane filter (Nexflo syringe filter, sterile,0.45 µm). TPGS and poloxamer P407 were used as a polymer and stabilizer respectively. Further, the same process was carried out for the preparation of Placebo nanomicelles without Dex. The obtained results from the AMTC system were quite promising with good reproducibility features having similar particle size and standard deviation when compared to the conventional method (Yu et al. 2015; Wang et al. 2016).

3.3 Electro-catalytic oxidation of uric acid and dopamine for NiO nanoparticles

Electro-catalytic-based detection of uric acid and dopamine with multi-walled carbon nanotube (MWCNT)–Nickel oxide nanostructures (MWCNT@NiO) were carried out in a 3-electrode system at neutral pH. Herein, 2B pencil graphite (PG) lead modified with MWCNT@NiO compound was used as a working electrode, Silver/silver chloride (Ag/AgCl) as a reference electrode, and platinum as a counter electrode. The working electrode was prepared by drop-casting 5 µl of MWCNT-ethanol suspension on PG, followed by air drying for 3 min. A 4 mg of NiO nanoparticle was added in 500 µl of ethanol and was sonicated for 6 min. 2 µl of the prepared NiO-ethanol suspension was coated on top of the

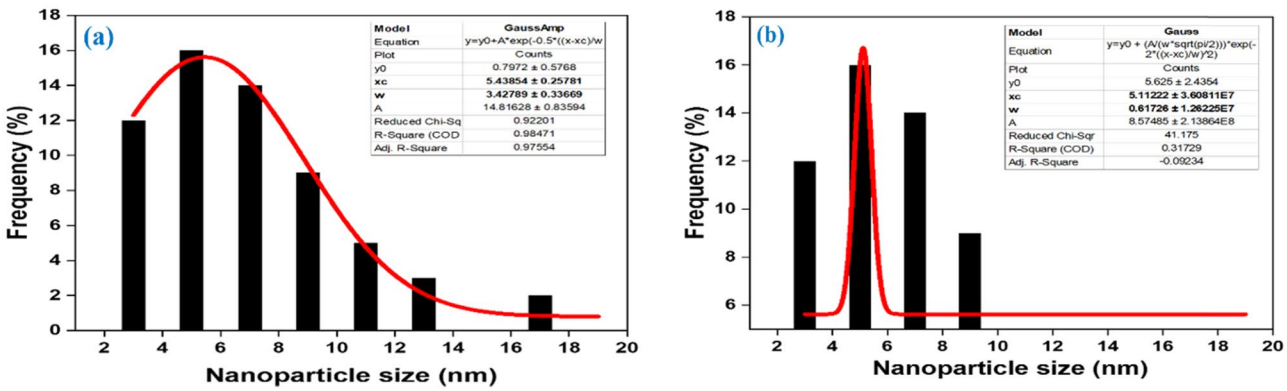

Fig. 8 (**a**) NiO nanoparticle size distribution curve (**b**) CuO nanoparticle size distribution curve

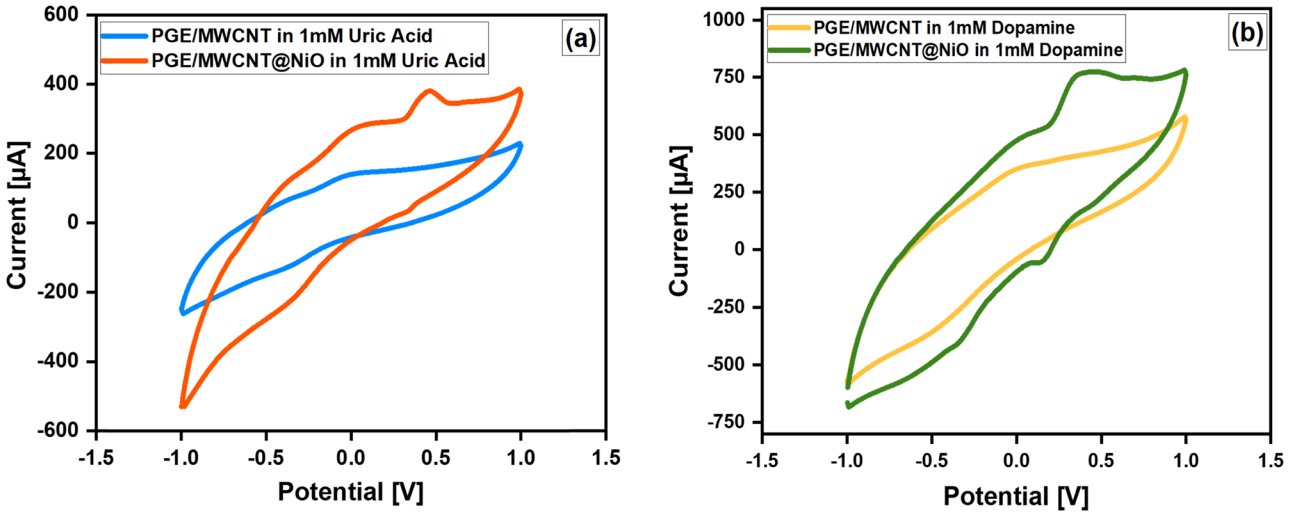

Fig. 9 (**a**) CV response of PGE/MWCNT and PGE/MWCNT@NiO in 1 mM Uric acid solution at 50 mV s^{-1} (**b**) CV response of PGE/MWCNT and PGE/MWCNT@NiO in 1 mM Dopamine (DA) solution at 50 mV s^{-1}

PGE/MWCNT to form PGE/MWCNT@NiO. The working electrode was kept for drying at 60 °C for 2 min in a hot air oven. The cyclic voltammetry technique was utilized at a scan rate of 50 mVs^{-1} in 1 mM of Uric acid and 1 mM dopamine. Figure 9a depicts that the blank electrode (PGE/MWCNT) alone gave no oxidation peak of uric acid whereas, PGE/MWCNT@NiO gave clear oxidation at E' = 0.43 V vs Ag/AgCl conforming to the oxidation of uric acid. Successively, it was identified that the produced NiO nanoparticles are electrochemically energetic and play a major role in the detection of uric acid.

Similarly, Fig. 9b shows the blank electrode (PGE/MWCNT) wherein, there was no oxidation peak was noticed. On the other hand, PGE/MWCNT@NiO provides a distinct oxidation peak at E' = 0.33 V vs Ag/AgCl electrode which is consistent with the oxidation peak indicating the detection of dopamine (DA).

3.4 Electro-catalytic oxidation of hydrazine and uric acid for CuO nanoparticles

The Electro-catalytic based detection of hydrazine with copper oxide nanostructures (PGE@CuO) was carried out in a 3-electrode system at neutral pH. Herein, 2B pencil graphite (PG) lead modified with CuO nanoparticles was used as a working electrode, Ag/AgCl as a reference, and platinum as a counter electrode. The working electrode was prepared by drop-casting 5 µl of CuO on PG and was kept for drying at

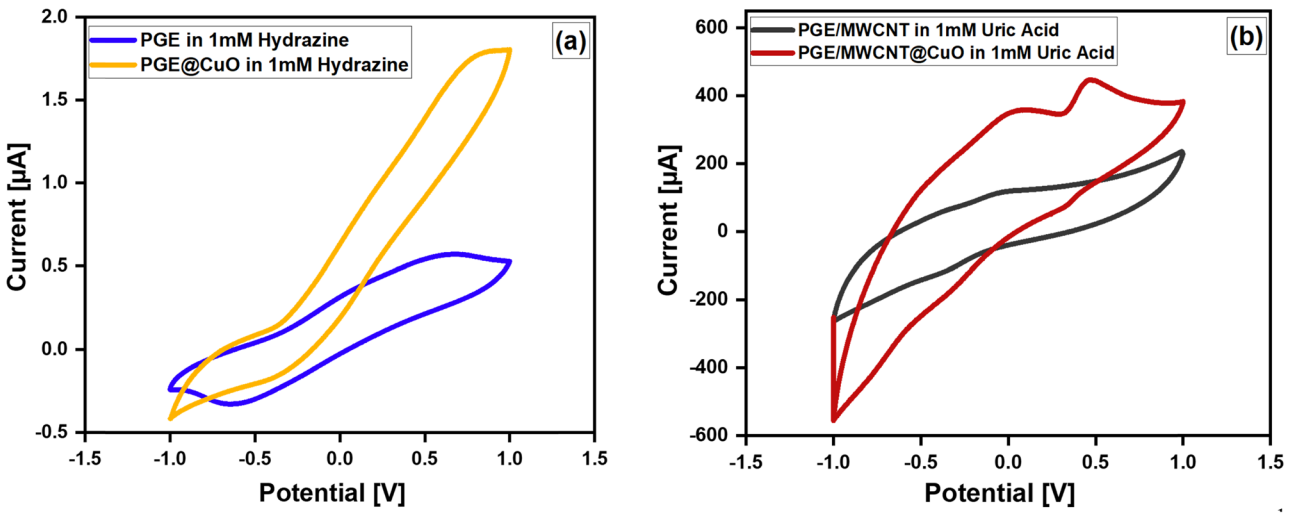

Fig. 10 (**a**) CV response of PGE and PGE@CuO in 1 mM hydrazine solution at 50 mV s^{-1} (**b**) CV response of PGE and PGE@CuO in 1 mM uric acid solution at 50 mV s^{-1}

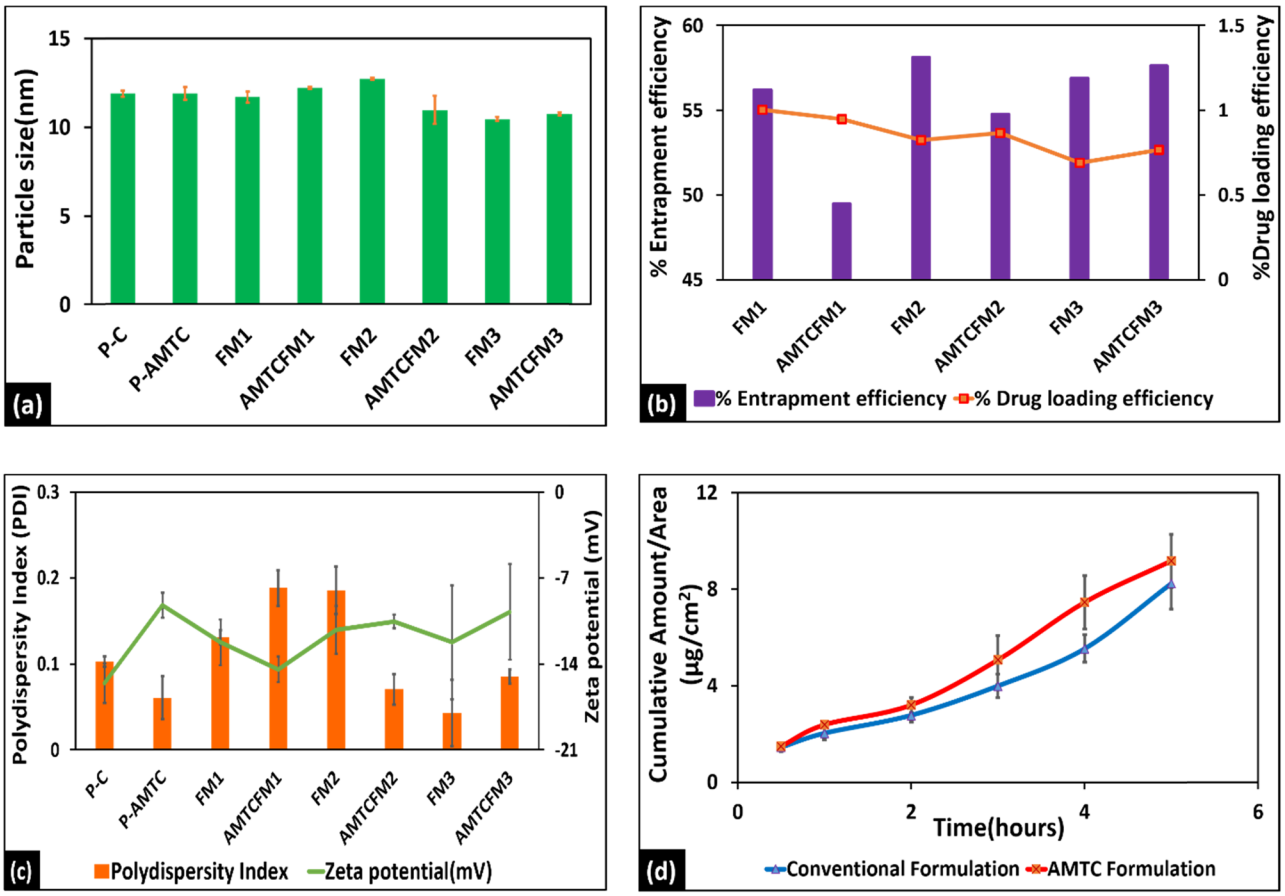

Fig. 11 Comparison of various evaluation parameters of 0.1% Dex-loaded Nanomicelles using Conventional and AMTC method. (**a**) Particle size distribution. (**b**) Entrapment efficiency and Drug loading efficiency. (**c**) Polydispersity index and Zeta potential. (**d**) Transcorneal penetration study. Note: P–C-Placebo Conventional; P-AMTC-Placebo Automated Temperature Control; FM-Formulation; AMTCFM- Automated Temperature Control Formulation

60 °C for 2 min in a hot air oven. The cyclic voltammetry technique was again harnessed at a scan rate of 50 mVs^{-1} in 1 mM of Uric acid and hydrazine. Figure 10a depicts that the blank electrode (PGE) alone gave no oxidation peak whereas, PG@CuO gave clear oxidation at E' = -0.35 V vs Ag/AgCl agreeing with the oxidation peak of hydrazine. Subsequently, it was known that CuO synthesized nanoparticles are electrochemically active and play an important role in hydrazine detection.

Likewise, Fig. 10b shows the blank electrode (PG) wherein, there was no oxidation peak observed in 1 mM solution of uric acid, while the PG@CuO provides a distinct oxidation peak at E' = 0.46 V vs Ag/AgCl electrode which is consistent with the electrocatalytic oxidation of uric acid. By further alteration, it can be used to fabricate an electrochemical sensor for uric acid and dopamine in real samples employing the microfluidic platform.

3.5 Evaluation of particle size, polydispersity index (PDI), zeta potential, and transcorneal penetration of 0.1% dex-loaded nanomicelles

The developed Dex-loaded nanomicelles were characterized for particle size, zeta potential, entrapment efficacy, drug loading, and transcorneal penetration studies. The entrapment efficacy and loading efficiency were determined by High-Pressure Liquid Chromatography (HPLC). Transcorneal studies were performed on the diffusion apparatus using goat cornea. Dex nanomicelles were optimized with a composition of Dex: TPGS (1:60 ratio). The mean diameter by conventional and AMTC based nanomicelles was found to be 10.45 ± 0.08 nm and 10.74 ± 0.08 nm, with a polydispersity index (PDI) of 0.043 and 0.085, respectively. Apparent permeability of 0.1% Dex-loaded nanomicelles using conventional and AMTC methods were 0.17217 and

0.18686 mm^2/hr respectively. Clear nanomicelles were obtained using both conventional and AMTC nanomicelles. The particle size distribution, polydispersity index, zeta potential, entrapment efficiency, drug loading efficiency, and transcorneal penetration of 0.1% Dex-loaded nanomicelles using conventional and AMTC methods were shown in Fig. 11a–d. The present study reveals that the Dex-loaded nanomicelles developed using the AMTC method were comparable to the conventional thin-film hydration method. The characterization parameters showed nanomicelles prepared using both methods showed promising results. The AMTC method is more cost-effective, consumes less power, standalone device, and requires less reaction time and drug sample as compared to the conventional thin-film hydration method.

4 Conclusion

The present work intends to synthesize the nanoparticles in a minuscule volume of samples which can be used for numerous biological, environmental, cosmetics and energy applications. Herein, the main focus was to design and develop a miniaturized, low-cost, easy-to-carry, simple temperature controller device using the arduino pro-mini platform which uses a proportional-derivative-integral (PID) concept for controlling the temperature. The minuscular device was completely integrated and automated on a PCB positioned in a 3D-printed housing. The thermal system showcased a temperature sensitivity of ± 2 °C. The real-time geotagged temperature data was made accessible through a smartphone with Bluetooth and IoT modules by installing an open-source app and stored for data analysis for a later stage. The complete portable device dimension comes with 100 (L) × 60 (W) × 32 mm^3 (H) respectively. The synthesis of nanoparticles in a miniaturized platform has its variety of sublime features such as precise temperature control, efficient mass and heat transfer, ambient ease, faster loading of samples, and overall safety. Herein, the nickel oxide and copper oxide nanoparticles and Dex loaded nanomicelles were synthesized on this proposed miniaturized device. In both the reaction samples, NiO was heated at 180 °C for 60 min and CuO was heated at 75 °C for 3 h respectively. Stringent characteristics, like FESEM and EDX, have been accomplished and analyzed which shows the formation of NiO and CuO nanoparticles. The obtained mean size of NiO and CuO nanostructures was 27.14 nm and 85.13 nm. In further, nanoparticles were employed for the electrocatalyst sensing of hydrazine, dopamine, and uric acid using the cyclic voltammetry technique. Furthermore, the study was conducted by loading Dex nanomicelles which were developed using an AMTC and compared to the conventional thin-film hydration method. The results showed a promising platform for the proposed method. The characterization parameters showed nanomicelles prepared using both methods are almost similar. Further, as a proof-of-concept, the developed nanomicelles were evaluated for transcorneal penetration using exvivo goat cornea model. The salient features of the proposed AMTC system are standalone, automated, low-cost, compact, miniaturized, low-power consumption, less reaction time and volume as compared to the conventional thin-film hydration method. In the future scope, this proposed method has the potential to accelerate the synthesis of nanoparticles and Dex loaded nanomicelles in a microfluidic platform.

Acknowledgements The authors would like to thank BITS-Pilani, Hyderabad campus for the infrastructural facility, the Central Analytical Laboratory (CAL) BITS-Pilani, Hyderabad Campus for the help provided in characterization techniques. Madhusudan B Kulkarni would like to thank Tata Consultancy Services (TCS) for providing a scholarship under TCS Research Scholar Program Cycle-15. Khairunnisa Amreen would like to acknowledge the NPDF scheme (PDF/2018/003658) for financial support. We would like to thank the Parenteral Drug Association, Indian Chapter for providing grant support to Nirmal J.

References

P.G. Jamkhande, N.W. Ghule, A.H. Bamer, M.G. Kalaskar, Metal Nanoparticles Synthesis: An Overview on Methods of Preparation, Advantages and Disadvantages, and Applications. J. Drug Deliv. Sci. Technol. **53**, 101174 (2019). https://doi.org/10.1016/j.jddst.2019.101174

M.J. Ndolomingo, N. Bingwa, R. Meijboom, Review of Supported Metal Nanoparticles: Synthesis Methodologies, Advantages and Application as Catalysts. J. Mater. Sci. **55**(15), 6195–6241 (2020). https://doi.org/10.1007/s10853-020-04415-x

Ealias, A.M. Saravanakumar, M. P. A Review on the Classification, Characterisation, Synthesis of Nanoparticles and Their Application. IOP Conf. Ser. Mater. Sci. Eng. **263**(3) (2017). https://doi.org/10.1088/1757-899X/263/3/032019

J.M. Mohan, K. Amreen, A. Javed, S.K. Dubey, S. Goel, Miniaturized Electrochemical Platform with Ink-Jetted Electrodes for Multiplexed and Interference Mitigated Biochemical Sensing. Appl. Nanosci. **10**(10), 3745–3755 (2020). https://doi.org/10.1007/s13204-020-01480-1

M.B. Kulkarni, S. Goel, Microfluidic Devices for Synthesizing Nanomaterials — a Review. Nano Express **1**(1), 1–30 (2020a)

N.S. Powar, V. Patel, Cu Nanoparticle: Synthesis, Characterization and Application Review Article Cu Nanoparticle: Synthesis, Characterization and Application. Chem. Methodol. **3,** 457–480 (2019). https://doi.org/10.22034/chemm.2019.154075.1112

S.J.R. Da. Silva, K. Pardee, L. Pena, Loop-Mediated Isothermal Amplification (LAMP) for the Diagnosis of Zika Virus: A Review. Viruses **12**(1), 1–20 (2019). https://doi.org/10.3390/v12010019

X. Wang, C. Hughes, S. Park, X. Ma, H.J. Cho, ZnO Nanoparticle-Based Optical Sensors Fabricated by High Current Density Electrodeposition and Flame Oxidation. Proc. IEEE Sensors **1**, 5–7 (2017). https://doi.org/10.1109/ICSENS.2016.7808843

S.B. Puneeth, M.B. Kulkarni, S. Goel, Microfluidic Viscometers for Biochemical and Biomedical Applications : A Review. Eng. Res. Express **3**, 1–29 (2021)

G. Yang, S.J. Park, Conventional and Microwave Hydrothermal Synthesis and Application of Functional Materials: A Review.

Materials (basel) **12**(21), 12–13 (2019). https://doi.org/10.3390/ma12213640

S. Ni, T. Li, X. Yang, Fabrication of NiO Nanoflakes and Its Application in Lithium Ion Battery. Mater. Chem. Phys. **132**(2–3), 1108–1111 (2012). https://doi.org/10.1016/j.matchemphys.2011.12.082

Li. Feng, L. Xuan, Z. Zhao, H. Bai, Y. Guo, J. Su, C. wei, X. Chen, MnO2 Prepared by Hydrothermal Method and Electrochemical Performance as Anode for Lithium-Ion Battery. Nanoscale Res. Lett. 9(1), 1–8 (2014). https://doi.org/10.1186/1556-276X-9-290

M. Li, W. Lei, Y. Yu, W. Yang, J. Li, D. Chen, S. Xu, M. Feng, H. Li, High-Performance Asymmetric Supercapacitors Based on Monodisperse MnO Nanocrystals with High Energy Densities. Nanoscale **10**(34), 15926–15931 (2018). https://doi.org/10.1039/c8nr04541k

U.S.J.S. Goel, Surface Modified 3D Printed Carbon Bioelectrodes for Glucose/O2 Enzymatic Biofuel Cell: Comparison and Optimization. Sustain. Energy Technol. Assessments. **42**, 100811 (2020). https://doi.org/10.1016/j.seta.2020.100811

D. Dector, D. Ortega-Díaz, J.M. Olivares-Ramírez, A. Dector, J.J. Pérez-Bueno, D. Fernández, D.M. Amaya-Cruz, A. Reyes-Rojas, Harvesting Energy from Real Human Urine in a Photo-Microfluidic Fuel Cell Using TiO2–Ni Anode Electrode. Int. J. Hydrogen Energy. xxxx, 1–11 (2021). https://doi.org/10.1016/j.ijhydene.2021.02.148

S. Thota, J. Kumar, Sol-Gel Synthesis and Anomalous Magnetic Behaviour of NiO Nanoparticles. J. Phys. Chem. Solids **68**(10), 1951–1964 (2007). https://doi.org/10.1016/j.jpcs.2007.06.010

R. Saravanan, N. Karthikeyan, V.K. Gupta, E. Thirumal, P. Thangadurai, V. Narayanan, A. Stephen, ZnO/Ag Nanocomposite: An Efficient Catalyst for Degradation Studies of Textile Effluents under Visible Light. Mater. Sci. Eng. C **33**(4), 2235–2244 (2013). https://doi.org/10.1016/j.msec.2013.01.046

C.T. Meneses, W.H. Flores, F. Garcia, J.M. Sasaki, A Simple Route to the Synthesis of High-Quality NiO Nanoparticles. J. Nanoparticle Res. **9**(3), 501–505 (2007). https://doi.org/10.1007/s11051-006-9109-2

S. Ekeroth, S. Ikeda, R.D. Boyd, T. Shimizu, U. Helmersson, Growth of Semi-Coherent Ni and NiO Dual-Phase Nanoparticles Using Hollow Cathode Sputtering. J. Nanoparticle Res. **21**(2), 1–8 (2019). https://doi.org/10.1007/s11051-019-4479-4

N. Chopra, L. Claypoole, L.G. Bachas, Morphological Control of Ni/NiO Core/Shell Nanoparticles and Production of Hollow NiO Nanostructures. J. Nanoparticle Res. **12**(8), 2883–2893 (2010). https://doi.org/10.1007/s11051-010-9879-4

K. Phiwdang, S. Suphankij, W. Mekprasart, W. Pecharapa, Synthesis of CuO Nanoparticles by Precipitation Method Using Different Precursors. Energy Procedia **34**, 740–745 (2013). https://doi.org/10.1016/j.egypro.2013.06.808

P. Pandey, S. Merwyn, G.S. Agarwal, B. K. Tripathi, S.C. Pant, Electrochemical Synthesis of Multi-Armed CuO Nanoparticles and Their Remarkable Bactericidal Potential against Waterborne Bacteria. J. Nanoparticle Res. 14(1) (2012). https://doi.org/10.1007/s11051-011-0709-0.

Q. Maqbool, S. Iftikhar, M. Nazar, F. Abbas, A. Saleem, T. Hussain, R. Kausar, S. Anwaar, N. Jabeen, Green Fabricated CuO Nanobullets via Olea Europaea Leaf Extract Shows Auspicious Antimicrobial Potential. IET Nanobiotechnol. **11**(4), 463–468 (2017). https://doi.org/10.1049/iet-nbt.2016.0125

G. Kesavan, S.M. Chen, Sonochemically Exfoliated Graphitic-Carbon Nitride for the Electrochemical Detection of Flutamide in Environmental Samples. Diam. Relat. Mater. **108**, 107975 (2020). https://doi.org/10.1016/j.diamond.2020.107975

A. Batool, S. Valiyaveettil, Co-Precipitation - An Efficient Method for Removal of Polymer Nanoparticles from Water. ACS Sustain. Chem. Eng. (2020). https://doi.org/10.1021/acssuschemeng.0c04511

M.B. Kulkarni, P.K. Yashas Enaganti, K. Amreen, S. Goel, Internet of Things Enabled Portable Thermal Management System with Microfluidic Platform to Synthesize MnO2 Nanoparticles for Electrochemical Sensing. Nanotechnology, **2020**, *31* (42), 1–8. https://doi.org/10.1088/1361-6528/ab9ed8.

R. Dobrucka, A. Romaniuk, D. Mariusz, Facile Synthesis of Au / ZnO / Ag Nanoparticles Using Glechoma Hederacea L . Extract , and Their Activity against Leukemia. Biomed. Microdevices, **2021**, 1–15. https://doi.org/10.1007/s10544-021-00557-0.

M. Li, L. Gu, T. Li, S. Hao, F. Tan, D. Chen, D. Zhu, Y. Xu, C. Sun, Z. Yang, Tio2-Seeded Hydrothermal Growth of Spherical Batio3 Nanocrystals for Capacitor Energy-Storage Application. Curr. Comput.-Aided Drug Des. **10**(3), 1–15 (2020). https://doi.org/10.3390/cryst10030202

Z. Qu, K. Wang, G. Alfranca, J.M. de la Fuente, D.A. Cui, Plasmonic Thermal Sensing Based Portable Device for Lateral Flow Assay Detection and Quantification. Nanoscale Res. Lett. 15(1) (2020). https://doi.org/10.1186/s11671-019-3240-3

W. Shi, N. Chopra, Surfactant-Free Synthesis of Novel Copper Oxide (CuO) Nanowire - Cobalt Oxide (Co3O4) Nanoparticle Heterostructures and Their Morphological Control. J. Nanoparticle Res. **13**(2), 851–868 (2011). https://doi.org/10.1007/s11051-010-0086-0

A.D. Vadlapudi, A.K. Mitra, Nanomicelles: An Emerging Platform for Drug Delivery to the Eye. Ther. Deliv. **4**(1), 1–3 (2013). https://doi.org/10.4155/tde.12.122

S. Patel, C. Garapati, P. Chowdhury, H. Gupta, J. Nesamony, S. Nauli, S.H.S. Boddu, Development and Evaluation of Dexamethasone Nanomicelles with Potential for Treating Posterior Uveitis after Topical Application. J. Ocul. Pharmacol. Ther. **31**(4), 215–227 (2015). https://doi.org/10.1089/jop.2014.0152

A.D. Vadlapudi, K. Cholkar, R.K. Vadlapatla, A.K. Mitra, Aqueous Nanomicellar Formulation for Topical Delivery of Biotinylated Lipid Prodrug of Acyclovir: Formulation Development and Ocular Biocompatibility. J. Ocul. Pharmacol. Ther. **30**(1), 49–58 (2014). https://doi.org/10.1089/jop.2013.0157

A. Patel, Ocular Drug Delivery Systems: An Overview. World J. Pharmacol. **2**(2), 47 (2013). https://doi.org/10.5497/wjp.v2.i2.47

N. Omerovi, E. Vrani, Application of Nanoparticles in Ocular Drug Delivery Systems. 61–78 (2020)

M. Alami-Milani, P. Zakeri-Milani, H. Valizadeh, S. Sattari, S. Salatin, M. Jelvehgari, Evaluation of Anti-Inflammatory Impact of Dexamethasone-Loaded PCL-PEG-PCL Micelles on Endotoxin-Induced Uveitis in Rabbits. Pharm. Dev. Technol. **24**(6), 680–688 (2019). https://doi.org/10.1080/10837450.2019.1578370

V. Gote, S. Sikder, J. Sicotte, D. Pal, Ocular Drug Delivery: Present Innovations and Future Challenges. J. Pharmacol. Exp. Ther. **370**(3), 602–624 (2019). https://doi.org/10.1124/jpet.119.256933

S.S. Chrai, M.C. Makoid, S.P. Eriksen, J.R. Robinson, Drop Size and Initial Dosing Frequency Problems of Topically Applied Ophthalmic Drugs. J. Pharm. Sci. **63**(3), 333–338 (1974). https://doi.org/10.1002/jps.2600630304

J. Nirmal, S.B. Singh, N.R. Biswas, V. Thavaraj, R.V. Azad, T. Velpandian, Potential Pharmacokinetic Role of Organic Cation Transporters in Modulating the Transcorneal Penetration of Its Substrates Administered Topically. Eye **27**(10), 1196–1203 (2013a). https://doi.org/10.1038/eye.2013.146

J. Nirmal, A. Sirohiwal, S.B. Singh, N.R. Biswas, V. Thavaraj, R.V. Azad, T. Velpandian, Role of Organic Cation Transporters in the Ocular Disposition of Its Intravenously Injected Substrate in Rabbits: Implications for Ocular Drug Therapy. Exp. Eye Res. **116**, 27–35 (2013b). https://doi.org/10.1016/j.exer.2013.07.004

C. Chaipan, A. Pryszlak, H. Dean, P. Poignard, V. Benes, A.D. Griffiths, C.A. Merten, Single-Virus Droplet Microfluidics for High-Throughput

Screening of Neutralizing Epitopes on HIV Particles. Cell Chem. Biol. **24**(6), 751-757.e3 (2017). https://doi.org/10.1016/j.chembiol.2017.05.009

M.B. Kulkarni, S. Goel, Advances in Continuous-Flow Based Microfluidic PCR Devices – A Review. Eng. Res. Express. 2(4), 0–21 (2020). https://doi.org/10.1088/2631-8695/abd287

M.M. Islam, A. Loewen, P.B. Allen, Simple, Low-Cost Fabrication of Acrylic Based Droplet Microfluidics and Its Use to Generate DNA-Coated Particles. Sci. Rep. **8**(1), 1–11 (2018). https://doi.org/10.1038/s41598-018-27037-5

X.C. Jiang, W.M. Chen, C.Y. Chen, S.X. Xiong, A.B. Yu, Role of Temperature in the Growth of Silver Nanoparticles Through a Synergetic Reduction Approach. Nanoscale Res. Lett. **6**(1), 1–9 (2011). https://doi.org/10.1007/s11671-010-9780-1

H. Liu, H. Zhang, J. Wang, J. Wei, Effect of Temperature on the Size of Biosynthesized Silver Nanoparticle: Deep Insight into Microscopic Kinetics Analysis. Arab. J. Chem. **13**(1), 1011–1019 (2020). https://doi.org/10.1016/j.arabjc.2017.09.004

R. Sigwadi, S. Dhlamini, T. Mokrani, P. Nonjola, Effect of Synthesis Temperature on Particles Size and Morphology of Zirconium Oxide Nanoparticle. J. Nano Res. **50**, 18–31 (2017)

N. Kamaly, Z. Xiao, P.M. Valencia, A.F. Radovic-Moreno, O.C. Farokhzad, Targeted Polymeric Therapeutic Nanoparticles: Design, Development and Clinical Translation. Chem. Soc. Rev. **41**(7), 2971–3010 (2012). https://doi.org/10.1039/c2cs15344k

N.H.A. Hamid, M.M. Kamal, F.H. Yahaya, Application of PID Controller in Controlling Refrigerator Temperature. Proc. 5th Int. Colloq. Signal Process. Its Appl. CSPA **2009**(2009), 378–384 (2009). https://doi.org/10.1109/CSPA.2009.5069255

H.M. Asraf, K.A. Nur Dalila, A.W. Muhammad Hakim, R.H. Muhammad Faizzuan Hon, Development of Experimental Simulator via Arduino-Based PID Temperature Control System Using LabVIEW. J. Telecommun. Electron. Comput. Eng. **9**(1–5), 53–57 (2017)

J. Park, R.A. Martin, J.D. Kelly, J.D. Hedengren, Benchmark Temperature Microcontroller for Process Dynamics and Control. Comput. Chem. Eng. **135**, 106736 (2020). https://doi.org/10.1016/j.compchemeng.2020.106736

J.L. Wang, Y.Q. Li, Y.J. Byon, S.G. Mei, G.L. Zhang, Synthesis and Characterization of NiTiO3 Yellow Nano Pigment with High Solar Radiation Reflection Efficiency. Powder Technol. **235**, 303–306 (2013). https://doi.org/10.1016/j.powtec.2012.10.044

H.F. Lu, R.Y. Hong, H.Z. Li, Influence of Surfactants on Co-Precipitation Synthesis of Strontium Ferrite. J. Alloys Compd. **509**(41), 10127–10131 (2011). https://doi.org/10.1016/j.jallcom.2011.08.058

Q. Yan, Y. Lu, F. To, Y. Li, F. Yu, Synthesis of Tungsten Carbide Nanoparticles in Biochar Matrix as a Catalyst for Dry Reforming of Methane to Syngas. Catal. Sci. Technol. **5**(6), 3270–3280 (2015). https://doi.org/10.1039/c5cy00029g

W. Lee, C.H. Bin Weng, F.Y. Cheng, C.S. Yeh, H.Y. Lei, G. Lee Bin, Biomedical Microdevices Synthesis of Iron Oxide Nanoparticles Using a Microfluidic System. Biomed. Microdevices. **11**(1), 161–171 (2009). https://doi.org/10.1007/s10544-008-9221-4

A.M. Nightingale, J.C. De. Mello, Controlled Synthesis of III-V Quantum Dots in Microfluidic Reactors. ChemPhysChem **10**(15), 2612–2614 (2009). https://doi.org/10.1002/cphc.200900462

T. Nakayama, Y. Kurosawa, S. Furui, K. Kerman, M. Kobayashi, S.R. Rao, Y. Yonezawa, K. Nakano, A. Hino, S. Yamamura et al., Circumventing Air Bubbles in Microfluidic Systems and Quantitative Continuous-Flow PCR Applications. Anal. Bioanal. Chem. **386**(5), 1327–1333 (2006). https://doi.org/10.1007/s00216-006-0688-7

M.B. Kulkarni, P.K. Enaganti, K. Amreen, S. Goel, Integrated Temperature Controlling Platform to Synthesize ZnO Nanoparticles and Its Deposition on Al-Foil For. IEEE Sens. J. **21**(7), 9538–9545 (2021). https://doi.org/10.1109/JSEN.2021.3053642

K. Cholkar, S. Hariharan, S. Gunda, A.K. Mitra, Optimization of Dexamethasone Mixed Nanomicellar Formulation. Ageing Int. **15**(6), 1454–1467 (2014). https://doi.org/10.1208/s12249-014-0159-y

A. Mandal, K. Cholkar, V. Khurana, A. Shah, V. Agrahari, R. Bisht, D. Pal, A.K. Mitra, Topical Formulation of Self-Assembled Antiviral Prodrug Nanomicelles for Targeted Retinal Delivery. Mol. Pharm. **14**(6), 2056–2069 (2017). https://doi.org/10.1021/acs.molpharmaceut.7b00128

T. Velpandian, J. Nirmal, H.P. Sharma, S. Sharma, N. Sharma, N. Halder, Novel Water Soluble Sterile Natamycin Formulation (Natasol) for Fungal Keratitis. Eur. J. Pharm. Sci. **163**, 635–105857 (2021). https://doi.org/10.1016/j.ejps.2021.105857

M. Wardani, Y. Yulizar, I. Abdullah, D.O. Bagus Apriandanu, Synthesis of NiO Nanoparticles via Green Route Using Ageratum Conyzoides L. Leaf Extract and Their Catalytic Activity. IOP Conf. Ser. Mater. Sci. Eng. **509**(1) (2019). https://doi.org/10.1088/1757-899X/509/1/012077

J. A. Singh, Brief Review on Synthesis and Characterization of Copper Oxide Nanoparticles and Its Applications. J. Bioelectron. Nanotechnol. **2016**, *1* (1), 1–9. https://doi.org/10.13188/2475-224x.1000003.

J. Yu, Y. Zhou, W. Chen, J. Ren, L. Zhang, L. Lu, G. Luo, H. Huang, Preparation, Characterization and Evaluation of α-Tocopherol Succinate-Modified Dextran Micelles as Potential Drug Carriers. Materials (basel) **8**(10), 6685–6696 (2015). https://doi.org/10.3390/ma8105332

Q. Wang, J. Jiang, W. Chen, H. Jiang, Z. Zhang, X. Sun, Targeted Delivery of Low-Dose Dexamethasone Using PCL-PEG Micelles for Effective Treatment of Rheumatoid Arthritis. J. Control. Release **230**, 64–72 (2016). https://doi.org/10.1016/j.jconrel.2016.03.035